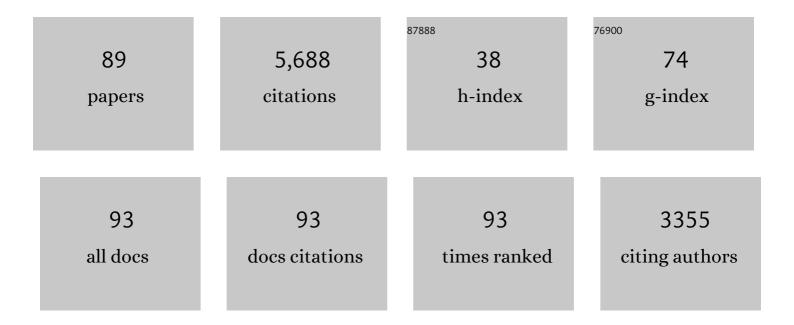
John A Mavrogenes

List of Publications by Year in descending order

Source: https://exaly.com/author-pdf/509223/publications.pdf Version: 2024-02-01



#	Article	IF	CITATIONS
1	Resolving sub-micrometer-scale zonation of trace elements in quartz using TOF-SIMS. American Mineralogist, 2022, 107, 955-969.	1.9	1
2	In situ elemental and Sr-Nd isotopic compositions of hydrothermal apatite from the Shazhou U deposit in the Xiangshan complex: Implications for the origins of ore-forming fluids of volcanic related U deposits in South China. Journal of Asian Earth Sciences, 2022, 233, 105230.	2.3	4
3	Fluid compositions reveal fluid nature, metal deposition mechanisms, and mineralization potential: An example at the Haobugao Zn-Pb skarn, China. Geology, 2021, 49, 473-477.	4.4	79
4	Compositions and Classification of Fractionated Boninite Series Melts from the Izu–Bonin–Mariana Arc: A Machine Learning Approach. Journal of Petrology, 2021, 62, .	2.8	6
5	Sources of auriferous fluids associated with a Neoarchean BIF-hosted orogenic gold deposit revealed by the multiple sulfur isotopic compositions of zoned pyrites. Contributions To Mineralogy and Petrology, 2021, 176, 1.	3.1	2
6	Cationic substitutions in sphalerite from the Porgera mine, Papua New Guinea. Canadian Mineralogist, 2021, 59, 573-587.	1.0	1
7	Magmatic processes recorded in plagioclase and the geodynamic implications in the giant Shimensi W–Cu–Mo deposit, Dahutang ore field, South China. Journal of Asian Earth Sciences, 2021, 212, 104734.	2.3	3
8	Metallogenic ages and sulfur sources of the giant Dahutang W–Cu–Mo ore field, South China: Constraints from muscovite 40Ar/39Ar dating and in situ sulfur isotope analyses. Ore Geology Reviews, 2021, 134, 104141.	2.7	5
9	Complex REE systematics of carbonatites and weathering products from uniquely rich Mount Weld REE deposit, Western Australia. Ore Geology Reviews, 2021, 139, 104539.	2.7	18
10	The sign of Δ33S is independent of pyrite morphology. Chemical Geology, 2020, 532, 119369.	3.3	1
11	Rare earth element mobility in and around carbonatites controlled by sodium, potassium, and silica. Science Advances, 2020, 6, .	10.3	96
12	Fluid properties and origins of the Lannigou Carlin-type gold deposit, SW China: Evidence from SHRIMP oxygen isotopes and LA-ICP-MS trace element compositions of hydrothermal quartz. Journal of Geochemical Exploration, 2020, 215, 106546.	3.2	14
13	Noble metal nanonugget insolubility in geological sulfide liquids. Geology, 2020, 48, 939-943.	4.4	20
14	Quadruple sulfur isotopic fractionation during pyrite desulfidation to pyrrhotite. Geochimica Et Cosmochimica Acta, 2020, 273, 354-366.	3.9	9
15	The Fluorapatite P–REE–Th Vein Deposit at Nolans Bore: Genesis by Carbonatite Metasomatism. Journal of Petrology, 2020, 61, .	2.8	44
16	Evolution of chalcophile elements in the magmas of the Bonin Islands. Chemical Geology, 2019, 508, 234-249.	3.3	13
17	Metallogeny of the Zoujiashan uranium deposit in the Mesozoic Xiangshan volcanic-intrusive complex, southeast China: Insights from chemical compositions of hydrothermal apatite and metal elements of individual fluid inclusions. Ore Geology Reviews, 2019, 113, 103085.	2.7	23
18	Geology and Genesis of the Giant Pulang Porphyry Cu-Au District, Yunnan, Southwest China. Economic Geology, 2019, 114, 275-301.	3.8	42

JOHN A MAVROGENES

#	Article	IF	CITATIONS
19	Petrogenesis and metallogenic significance of multistage granites in Shimensi tungsten polymetallic deposit, Dahutang giant ore field, South China. Lithos, 2019, 336-337, 326-344.	1.4	17
20	Significance of high temperature fluids and melts in the Grasberg porphyry copper‑gold deposit. Chemical Geology, 2019, 508, 210-224.	3.3	21
21	Carbonatitic versus hydrothermal origin for fluorapatite REE-Th deposits: Experimental study of REE transport and crustal "antiskarn―metasomatism. Numerische Mathematik, 2018, 318, 335-366.	1.4	48
22	Silicate-sulfide liquid immiscibility in modern arc basalt (Tolbachik volcano, Kamchatka): Part I. Occurrence and compositions of sulfide melts. Chemical Geology, 2018, 478, 102-111.	3.3	38
23	REE Redistribution Textures in Altered Fluorapatite: Symplectites, Veins, and Phosphate-Silicate-Carbonate Assemblages from the Nolans Bore P-REE-Th Deposit, Northern Territory, Australia. Canadian Mineralogist, 2018, 56, 331-354.	1.0	35
24	Crustal sequestration of magmatic sulfur dioxide. Geology, 2017, 45, 211-214.	4.4	20
25	Trace element and sulfur isotopic evidence for redox changes during formation of the Wallaby Gold Deposit, Western Australia. Ore Geology Reviews, 2017, 82, 31-48.	2.7	42
26	Platinum-group elements and gold in sulfide melts from modern arc basalt (Tolbachik volcano,) Tj ETQq0 0 0 rgB	3T /Oyerloc I.4	:k 10 Tf 50 46
27	Effect of S on the aqueous and gaseous transport of Cu in porphyry and epithermal systems: Constraints from in situ XAS measurements up to 600 °C and 300 bars. Chemical Geology, 2017, 466, 500-511.	3.3	14
28	Sulfur isotope and trace element systematics of zoned pyrite crystals from the El Indio Au–Cu–Ag deposit, Chile. Contributions To Mineralogy and Petrology, 2016, 171, 1.	3.1	82
29	A synthetic fluid inclusion study of the solubility of monazite-(La) and xenotime-(Y) in H2O-Na-K-Cl-F-CO2 fluids at 800 °C and 0.5 GPa. Chemical Geology, 2016, 442, 121-129.	3.3	25
30	Experimental observations on noble metal nanonuggets and Fe-Ti oxides, and the transport of platinum group elements in silicate melts. Geochimica Et Cosmochimica Acta, 2016, 192, 258-278.	3.9	30
31	Nb-Ta fractionation in peraluminous granites: A marker of the magmatic-hydrothermal transition: COMMENT. Geology, 2016, 44, e394-e394.	4.4	18
32	The competing effects of sulfide saturation versus degassing on the behavior of the chalcophile elements during the differentiation of hydrous melts. Geochemistry, Geophysics, Geosystems, 2015, 16, 1490-1507.	2.5	57
33	Generation of porphyry copper deposits by gas–brine reaction in volcanic arcs. Nature Geoscience, 2015, 8, 235-240.	12.9	154
34	Hydrothermal controls on the genesis of REE deposits: Insights from an in situ XAS study of Yb solubility and speciation in high temperature fluids (T < 400 ŰC). Chemical Geology, 2015, 417, 228-237.	3.3	26
35	The Effect of FeO on the Sulfur Content at Sulfide Saturation (SCSS) and the Selenium Content at Selenide Saturation of Silicate Melts. Journal of Petrology, 2015, 56, 1407-1424.	2.8	57
36	Silica hydrate preserved with δ180-rich quartz in high-temperature hydrothermal quartz in the high sulfidation copper-gold deposit at El Indio, Chile. Chemical Geology, 2015, 391, 90-99.	3.3	6

JOHN A MAVROGENES

#	Article	IF	CITATIONS
37	Trace Element Stratigraphy of the Bellevue Core, Northern Bushveld: Multiple Magma Injections Obscured by Diffusive Processes. Journal of Petrology, 2014, 55, 859-882.	2.8	39
38	The key role of mica during igneous concentration of tantalum. Contributions To Mineralogy and Petrology, 2014, 167, 1.	3.1	211
39	Linking high-grade gold mineralization to earthquake-induced fault-valve processes in the Porgera gold deposit, Papua New Guinea. Geology, 2014, 42, 383-386.	4.4	138
40	Combining in situ isotopic, trace element and textural analyses of quartz from four magmatic-hydrothermal ore deposits. Contributions To Mineralogy and Petrology, 2013, 166, 1119-1142.	3.1	43
41	EXPERIMENTAL EVIDENCE OF SULFIDE MELT EVOLUTION VIA IMMISCIBILITY AND FRACTIONAL CRYSTALLIZATION. Canadian Mineralogist, 2013, 51, 841-850.	1.0	15
42	The Magnetite Crisis in the Evolution of Arc-related Magmas and the Initial Concentration of Au, Ag and Cu. Journal of Petrology, 2012, 53, 1089-1089.	2.8	5
43	Sulfosalt melts and heavy metal (Asâ€Sbâ€Biâ€Snâ€Pbâ€Tl) fractionation during volcanic gas expansion: the El Indio (Chile) paleoâ€fumarole. Geofluids, 2012, 12, 199-215.	0.7	22
44	Chalcophile element systematics in volcanic glasses from the northwestern Lau Basin. Geochemistry, Geophysics, Geosystems, 2012, 13, .	2.5	81
45	Ti site occupancy in zircon. Geochimica Et Cosmochimica Acta, 2011, 75, 905-921.	3.9	72
46	Textural Evidence for Extensive Melting of the Broken Hill Orebody. Economic Geology, 2011, 106, 869-882.	3.8	15
47	Geology and Intrusion-Related Affinity of the Morila Gold Mine, Southeast Mali. Economic Geology, 2011, 106, 727-750.	3.8	66
48	The Magnetite Crisis in the Evolution of Arc-related Magmas and the Initial Concentration of Au, Ag and Cu. Journal of Petrology, 2010, 51, 2445-2464.	2.8	351
49	SULFOSALT MELTS: EVIDENCE OF HIGH-TEMPERATURE VAPOR TRANSPORT OF METALS IN THE FORMATION OF HIGH-SULFIDATION LODE GOLD DEPOSITS. Economic Geology, 2010, 105, 257-262.	3.8	36
50	Tungsten isotopes as tracers of core–mantle interactions: The influence of subducted sediments. Geochimica Et Cosmochimica Acta, 2010, 74, 751-762.	3.9	18
51	Controls on gold solubility in arc magmas: An experimental study at 1000°C and 4kbar. Geochimica Et Cosmochimica Acta, 2010, 74, 2165-2189.	3.9	45
52	Determination of Selenium Concentrations in NIST SRM 610, 612, 614 and Geological Glass Reference Materials Using the Electron Probe, LAâ€ICPâ€MS and SHRIMP II. Geostandards and Geoanalytical Research, 2009, 33, 309-317.	3.1	15
53	The effect of CO2 on the speciation of RbBr in solution at temperatures to 579°C and pressures to 0.26GPa. Geochimica Et Cosmochimica Acta, 2009, 73, 2631-2644.	3.9	10
54	XANES evidence for sulphur speciation in Mn-, Ni- and W-bearing silicate melts. Geochimica Et Cosmochimica Acta, 2009, 73, 6847-6867.	3.9	18

#	Article	IF	CITATIONS
55	Petrogenesis of contact-style PCE mineralization in the northern lobe of the Bushveld Complex: comparison of data from the farms Rooipoort, Townlands, Drenthe and Nonnenwerth. Mineralium Deposita, 2008, 43, 255-280.	4.1	52
56	The importance of talc and chlorite "hybrid―rocks for volatile recycling through subduction zones; evidence from the high-pressure subduction mélange of New Caledonia. Contributions To Mineralogy and Petrology, 2008, 155, 181-198.	3.1	148
57	A preliminary investigation of chlorine XANES in silicate glasses. Geochemistry, Geophysics, Geosystems, 2008, 9, .	2.5	34
58	An experimental study of the solubility of molybdenum in H2O and KCl–H2O solutions from 500 °C to 800 °C, and 150 to 300 MPa. Geochimica Et Cosmochimica Acta, 2008, 72, 2316-2330.	3.9	147
59	Sulphur solubility and sulphide immiscibility in silicate melts as a function of the concentration of manganese, nickel, tungsten and copper at 1Âatm and 1400°C. Chemical Geology, 2008, 255, 236-249.	3.3	20
60	Mineral solubility and hydrous melting relations in the deep earth: Analysis of some binary A H2O system pressure-temperature-composition topologies. Numerische Mathematik, 2007, 307, 833-855.	1.4	24
61	Experimental constraints on element mobility from subducted sediments using high-P synthetic fluid/melt inclusions. Chemical Geology, 2007, 239, 228-249.	3.3	171
62	Recognizing hydrothermal alteration through a granulite facies metamorphic overprint at the challenger Au deposit, South Australia. Chemical Geology, 2007, 243, 64-89.	3.3	27
63	The effect of CO2on the speciation of bromine in low-temperature geological solutions: an XANES study. Journal of Synchrotron Radiation, 2007, 14, 219-226.	2.4	12
64	A XANES study of Cu speciation in high-temperature brines using synthetic fluid inclusions. American Mineralogist, 2006, 91, 1773-1782.	1.9	56
65	A synthetic fluid inclusion study of copper solubility in hydrothermal brines from 525 to 725°C and 0.3 to 1.7GPa. Geochimica Et Cosmochimica Acta, 2006, 70, 3970-3985.	3.9	45
66	A cold-sealing capsule design for synthesis of fluid inclusions and other hydrothermal experiments in a piston-cylinder apparatus. American Mineralogist, 2006, 91, 203-210.	1.9	20
67	SULFIDE MELT INCLUSIONS AS EVIDENCE FOR THE EXISTENCE OF A SULFIDE PARTIAL MELT AT BROKEN HILL, AUSTRALIA. Economic Geology, 2005, 100, 773-779.	3.8	38
68	HYDROUS SULFIDE MELTING: EXPERIMENTAL EVIDENCE FOR THE SOLUBILITY OF H2OIN SULFIDE MELTS. Economic Geology, 2005, 100, 157-164.	3.8	37
69	Origin of chromitites in layered intrusions: Evidence from chromite-hosted melt inclusions from the Stillwater Complex. Geology, 2005, 33, 893.	4.4	133
70	Reply to comments on "Redistribution of trace elements during prograde metamorphism from lawsonite blueschist to eclogite facies: implications for deep subduction zone processes― Contributions To Mineralogy and Petrology, 2004, 148, 506-509.	3.1	3
71	Geochronological constraints on the polymetamorphic evolution of the granulite-hosted Challenger gold deposit: implications for assembly of the northwest Gawler Craton*. Australian Journal of Earth Sciences, 2004, 51, 1-14.	1.0	32
72	Geochemical heterogeneity and element mobility in deeply subducted oceanic crust; insights from high-pressure mafic rocks from New Caledonia. Chemical Geology, 2004, 206, 21-42.	3.3	154

#	Article	IF	CITATIONS
73	Petrogenesis of the Greenhills Complex, Southland, New Zealand: magmatic differentiation and cumulate formation at the roots of a Permian island-arc volcano. Contributions To Mineralogy and Petrology, 2003, 144, 703-721.	3.1	69
74	Redistribution of trace elements during prograde metamorphism from lawsonite blueschist to eclogite facies; implications for deep subduction-zone processes. Contributions To Mineralogy and Petrology, 2003, 146, 205-222.	3.1	322
75	Generation of metal-rich felsic magmas during crustal anatexis. Geology, 2003, 31, 765.	4.4	39
76	The Sulfide Capacity and the Sulfur Content at Sulfide Saturation of Silicate Melts at 1400degreesC and 1 bar. Journal of Petrology, 2002, 43, 1049-1087.	2.8	336
77	Copper speciation in vapor-phase fluid inclusions from the Mole Granite, Australia. American Mineralogist, 2002, 87, 1360-1364.	1.9	55
78	Mobilization of Gold as a Polymetallic Melt during PeliteAnatexis at the Challenger Deposit, South Australia: A MetamorphosedArchean Gold Deposit. Economic Geology, 2002, 97, 1249-1271.	3.8	36
79	PARTIAL MELTING OF SULFIDE ORE DEPOSITS DURING MEDIUM- AND HIGH-GRADE METAMORPHISM. Canadian Mineralogist, 2002, 40, 1-18.	1.0	183
80	Redistribution of Gold within Arsenopyrite and Lollingite during Pro- and Retrograde Metamorphism: Application to Timing of Mineralization. Economic Geology, 2001, 96, 525-534.	3.8	60
81	Partial melting of the Broken Hill Galena-Sphalerite ore: Experimental studies in the system PbS-FeS-ZnS-(Ag2S). Economic Geology, 2001, 96, 205-210.	3.8	78
82	Using melt inclusions to determine parent-magma compositions of layered intrusions: Application to the Greenhills Complex (New Zealand), a platinum group minerals–bearing, island-arc intrusion. Geology, 2000, 28, 991.	4.4	37
83	Using melt inclusions to determine parent-magma compositions of layered intrusions: Application to the Greenhills Complex (New Zealand), a platinum group minerals–bearing, island-arc intrusion. Geology, 2000, 28, 991-994.	4.4	1
84	Cold Solubility in Supercritical Hydrothermal Brines Measured in Synthetic Fluid Inclusions. Science, 1999, 284, 2159-2163.	12.6	198
85	The relative effects of pressure, temperature and oxygen fugacity on the solubility of sulfide in mafic magmas. Geochimica Et Cosmochimica Acta, 1999, 63, 1173-1180.	3.9	585
86	Comparison of decrepitation, microthermometric and compositional characteristics of fluid inclusions in barren and auriferous mesothermal quartz veins of the Cowra Creek Gold District, New South Wales, Australia. Journal of Geochemical Exploration, 1995, 54, 167-175.	3.2	16
87	Assessment of the uncertainties and limitations of quantitative elemental analysis of individual fluid inclusions using synchrotron X-ray fluorescence (SXRF). Geochimica Et Cosmochimica Acta, 1995, 59, 3987-3995.	3.9	54
88	Hydrogen movement into and out of fluid inclusions in quartz: Experimental evidence and geologic implications. Geochimica Et Cosmochimica Acta, 1994, 58, 141-148.	3.9	151
89	Mineralogy, paragenesis, and mineral zoning of the West Fork Mine, Virburnum Trend, Southeast Missouri. Economic Geology, 1992, 87, 113-124.	3.8	10